THE MAGNETIC PROPERTIES OF SPIN CROSSOVER MANGANESE(III) COMPOUNDS

M. A. Roman

Institute of Applied Physics, Academy of Sciences of Moldova, Academiei str. 5, Chisinau, MD-2028 Republic of Moldova

(Received 19 October 2011)

Abstract

A theoretical model to explain the phenomenon of spin crossover in the $[MnL2]NO_3$ compound is elaborated. The model takes into account the low symmetry crystal field acting on the manganese ion and the cooperative long-range electron-deformational interaction facilitating the spin transition. The range of the crystal field parameters for which the low-lying part of the energy spectrum of an isolated Mn^{III} ion consists of two orbitally non-degenerate levels with spins S=1 and 2 is determined. It is demonstrated that the S=1 state is the ground one in a narrow range of parameters. The *ls-hs* transition is considered as a cooperative phenomenon driven by the interaction of the electronic shells of the Mn^{III} ions with the all-round full symmetric deformation that is extended over the crystal lattice via the acoustic phonon field. Quite good agreement has been obtained between the calculated and experimental values of the magnetic susceptibility and the effective magnetic moment.

1. Introduction

The spin-crossover (SCO) phenomenon refers to the transitions between high-spin (*hs*) to low spin (*ls*) or *ls* to *hs* states in octahedral transition metal complexes with d^4,d^5,d^6 and d^7 electronic configurations. The spin transition can be triggered by external stimuli, such as temperature, pressure, and electromagnetic radiation, and it is associated with the switching of other properties, such as the color, paramagnetism, dielectric constant, and conductivity [1, 2]. However, the two most important consequences of a spin transition are the observed: changes in the metal-donor atom distance due to the change in the relative occupancies of the t_2 and e orbitals and the changes in magnetic properties. Thus, due to their properties, spin crossover compounds present one of the best examples of molecular bistability and can be proposed for several technological applications as elements of molecular memory, sensors, and displays [1, 3]. Since SCO phenomenon was discovered by Cambi et al. more than 70 years ago in a series of Fe^{III} tris-dithiocarbamate compounds [4-6], numerous other compounds exhibiting this phenomenon in the solid state and in solution have been reported. Most of them are compounds of Fe^{II} ($3d^6$), Fe^{III} ($3d^5$) and Co^{II} ($3d^7$) [7-12] and only in few cases this phenomenon is observed for Cr^{II} and Mn^{III} ($3d^4$) [13-16] compounds. The manganese(III) compound obtained in 1981 represented the first d^4 SCO system [17]. A well-characterized example of spin conversion in Mn^{III} ions [13] also represents the [Mn(trp)] (trp^{3-} =tris{1-(2-azolyl)-2-azabuten-4-yl}amine) which continues to attract attention of researchers [18-20]. The [Mn(taa)](H_3taa=tris(1-(2-azolyl)-2-azabuten-4-yl)amine) compound in the cubic crystalline form is also known to exhibit an abrupt $^5E \leftrightarrow {}^3T_1$ spin crossover phase transition at 48 K. The

paraelectric behavior due to a dynamic Jahn-Teller effect has been found for this compound in the *hs* phase above $T_c = 48K$ [2]. At the same time, the dielectric constant of the compound obeys the Curie-Weiss law with an asymptotic Curie temperature of 26 K, suggesting competition between the ls phase and a ferroelectric-ordered phase at low temperatures.

Recently, it was observed that modulation of the orientation of the N4(O-)2 donors in a series of hexadentate ligands has a dramatic effect on the spin state of Mn^{III} complexes and that gradual thermal spin-crossover may be attained when the phenolate oxygen donors are trans to each other [21]. In fact, by variation the length of the alkyl chains in the starting tetramine, this geometry was achieved. A manganese(III) complex possessing a ground hs state at all temperatures was obtained with the aid of a triethylene-tetraamine link (L1) which orients the oxygen donors cis to each other. At the same time, the lengthening of the tetraamine link by two methylene groups (L2) led to a trans geometry of the oxygen donors facilitating the spin crossover [21] in the [MnL2]NO3 compound.

The manganese(III) SCO compounds have been intensively studied last years by theoreticians. In [2, 22, 23] the DFT method was successfully applied. In [2] the geometry optimization of the hs [Mn(taa)] molecule was carried out by a hybrid DFT quantum chemical calculation. Based on a four-state Ising-Potts model, a phase diagram incorporating both a virtual cooperative Jahn-Teller transition from the hs to the ferroelectrically ordered phase and a spin crossover transition $hs \leftrightarrow ls$ was proposed to elucidate the interrelation between these three phases of the [Mn(taa)] compound [2]. Three adjustable parameters were introduced in the model to reproduce the spin-crossover transition temperature, the virtual Jahn-Teller transition temperature, and the effective ls-hs gap. Meanwhile, in [2] the interion interactions are introduced phenomenologically within the framework of the 4-state Ising-Potts model. In [22] with the aid of DFT for the [Mn(5-Br-sal-N-1,5,8,12)]ClO_4 complex, the geometry optimization and vibration analysis were performed, the spin and density difference maps were obtained. From DFT calculations, the parameters relevant for the interpretation of the observed effect in the framework of the ligand-field paradigm were retrieved [22]. It was found that the *hs* ground state is higher by $\Delta E \sim 2000 cm^{-1}$ than the *ls* one.

In the present paper, we develop a microscopic theoretical approach to the SCO phenomenon in crystals containing manganese(III) ions as structural units and reveal the main mechanisms governing this effect. With the aid of this approach, we explain the experimental data on the temperature dependence of the magnetic susceptibility and magnetic moment in the [MnL2]NO_3 compound [21].

2. The model

The Mn^{III} ion possesses 4 electrons in the incomplete *d*-shell. Depending on the ratio Dq/B in the cubic crystal field (where Dq is the parameter of the cubic crystal field and B is the Racah parameter), the ground state of this ion is the triplet $^3T_1$ or the doublet ^5E further on referred to as the *ls*- and *hs*-state, respectively. The interaction of the ground ^5E state of the Mn^{III} ion with the tetragonal Jahn-Teller vibrations of the high symmetrical ligand surrounding leads to the situation when the system is held up in one of the minimums of the lower adiabatic potential sheet that results in the distortion of the octahedral manganese complex and lowering of its symmetry [24]. The majority of *hs*- manganese(III) complexes subject to the Jahn-Teller effect demonstrate elongated octahedral surroundings. In this case, one inevitably faces the problem of

finding out the initial equilibrium configuration of the complex. Unfortunately, this problem cannot be solved in a unique way. Therefore, usually a simplified model is applied which assumes that the observed distortion of the Mn^{III} complexes is a result of action of a low symmetry crystal field.

Table 1. Spherical coordinates of the ligands in the MnN_4O_2 complex in the $[MnL2]NO_3$ compound

Ligand	1	2	3	4	5	6
R_i, Å	1.988	1.988	2.050	2.050	1.872	1.872
θ_i, r	$\frac{\pi}{2}$	$\frac{\pi}{2}$	$\frac{\pi}{2}$	$\frac{\pi}{2}$	0	π
φ_i,	0	$\frac{\pi}{2}$	π	$\frac{3\pi}{2}$	0	0

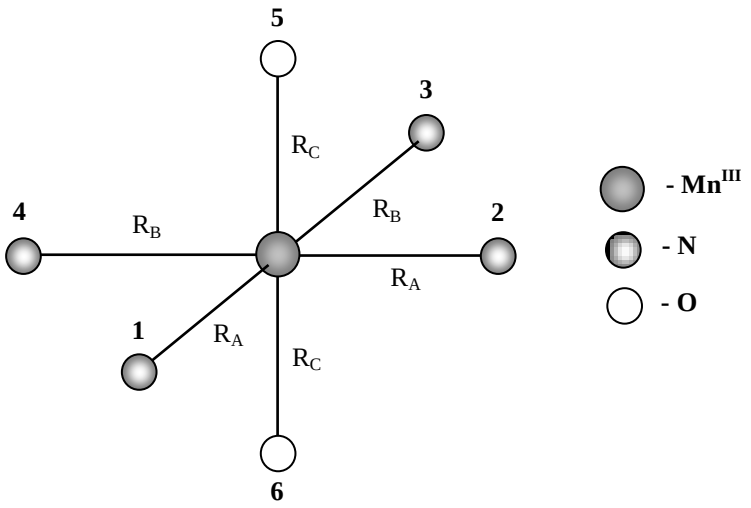

Fig. 1. Ligand surrounding of the Mn^{III} ion in the $[MnL2]NO_3$ compound.

Inspection of the molecular structure and interatomic distances (Table 1) reveals that, in the $[MnL2]NO_3$ [21] complex, the Mn^{III} ion has a quasi-octahedral environment made up by four nitrogen and two oxygen atoms (Fig. 1). With temperature rise, the Mn-N bond lengths increase, while the axial Mn-O bond lengths remain almost the same. In the temperature range of 100-300 K, the symmetry of the $[MnL2]NO_3$ complex [21] does not change and the complex may be approximately regarded as a system belonging to the C_{2v} point group. The structure of the $[MnL2]NO_3$ complex differs from that for manganese(III) complexes subject to strong Jahn-Teller effect because this complex is compressed along the O-Mn-O direction. This difference along with the conserved symmetry of the complex in a wide temperature range suggests that the cooperative interaction facilitating the spin transition is apparently not of Jahn-Teller nature. At the same time, in order to avoid the solution of the Jahn-Teller problem for an isolated complex, we assume that the distortion of the nearest surrounding of the Mn ion comes from a low symmetry crystal field.

The Hamiltonian of the system of interacting manganese ions

$$H = \sum_n V_{cr}^n + \sum_n V_{ee}^n + V_{st} \quad (1)$$

includes the crystal fields (V_{cr}^n) acting on the manganese ions, the electron-electron repulsion (V_{ee}^n) inside each manganese ion, and the electron-deformational cooperative interaction between the manganese ions which facilitates the spin transition.

2.1. Crystal field

We employ the exchange-charge model of the crystal field [25-30] that takes into account two contributions to the energy of the Mn^{III} ion in the crystal field, namely, the contribution arising from the interaction of the electrons in the d-shell with the point charges (pc) of the surrounding ligands and the contribution coming from the overlap of the 3d orbital with the ligand orbitals. The latter is referred to as the contribution of exchange charges (ec). In this model, the parameters B_l^m of the crystal field operator

$$V_{cr} = \sum_\alpha W\left(\left|\vec{r} - \vec{R}_{i\alpha}\right|\right) = \sum_{l,m} B_l^m Y_l^m(\vartheta, \varphi) \quad (2)$$

are represented as

$$B_l^m = B_l^{m(pc)} + B_l^{m(ec)}, \quad (3)$$

where $W(\left|\vec{r} - \vec{R}_{i\alpha}\right|)$ is the electron-nuclear potential energy , the component

$$B_l^{m(pc)} = \left(\frac{4\pi}{2l+1}\right) \sum_\alpha \frac{Z_\alpha e^2 < r^l >}{(R_\alpha)^{l+1}} Y_l^{m*}(\vartheta_\alpha, \varphi_\alpha) \quad (4)$$

is determined in the usual manner [26-30] and depends on the positions of the ligands, their effective charges and radial integrals $< r^l >$ for the manganese ions [31], $Y_{pm}(\vartheta, \varphi)$ are normalized spherical harmonics . The component $B_l^{m(ec)}$

$$B_l^{m(ec)} = \frac{8\pi e^2}{5} G \sum_\alpha \frac{S_l(R_\alpha)}{R_\alpha} Y_l^{m*}(\vartheta_\alpha, \varphi_\alpha) \quad (5)$$

is proportional to a linear combination of squares of different type overlap integrals of the 3d functions of the manganese ions and 2s,2p wave functions of the oxygen and nitrogen ligands

$$S_p(R_\alpha) = S_s^2(R_\alpha) + S_\sigma^2(R_\alpha) + \gamma_p S_\pi^2(R_\alpha) \quad \gamma_2 = 1, \gamma_4 = -4/3, \quad (6)$$

here $S_s(R_\alpha) = < 3d, m=0 | 2s >$, $S_\sigma(R_\alpha) = < 3d, m=0 | 2p, m=0 >$, $S_\pi(R_\alpha) = < 3d, m=\pm 1 | 2p, m=\pm 1 >$ are the overlap integrals of the 3*d* wave functions of manganese ions and 2*s*, 2*p* wave functions of the oxygen or nitrogen ligands, *G* is the phenomenological parameter of the model. For the Mn^{III} ions, the crystal field operator written in the frame of reference shown in Fig. 1 looks as follows

$$V_{cr} = B_2^0 Y_{2,0} + B_4^0 Y_{4,0} + B_4^4 (Y_{4,-4} + Y_{4,4}) \quad (7)$$

where the parameters B_l^m are determined as

$$B_2^0 = -\frac{4e^2\sqrt{\frac{\pi}{5}}}{R_A R_B R_C^3}\left(-R_A R_B\langle r^2\rangle + GR_C^2(R_B R_C S_2(R_A) + R_A R_C S_2(R_B) - 2R_A R_B S_2(R_C)\right)$$

$$B_4^0 = -\frac{e^2\sqrt{\pi}}{15 R_A R_B R_C^5}\left(40R_A R_B\langle r^4\rangle + 9GR_C^4(3R_B R_C S_4(R_A) + 3R_A R_C S_4(R_B) + 8R_A R_B S_4(R_C)\right)$$

$$B_4^4 = -\frac{3e^2 G\sqrt{\frac{7\pi}{10}}}{R_A R_B}\left(R_B S_4(R_A) + R_A S_4(R_B)\right). \qquad (8)$$

Expressions (8) were obtained taking into account that, in the compound under examination, the point charges of oxygen and nitrogen ligands are equal to *e* and 0, respectively; the spherical coordinates of the ligands are given in Table 1. In the subsequent calculations for the Mn^{III} ion, the values $< r^2 >= 1.286$ a.u., $< r^4 >= 3.446$ a.u. were used [31].

Table 2. Numerical values of the overlap integrals $S_l(R)$, their derivatives $S_l'(R)$ and crystal field parameters B_l^m as functions of the parameter G

$S_2(R_A)$	$S_4(R_A)$	$S_2(R_B)$	$S_4(R_B)$	$S_2(R_C)$	$S_4(R_C)$
0.0169	0.0107	0.0140	0.0091	0.0201	0.0128
$S_2'(R_A)$ (in a_0^{-1} *))	$S_4'(R_A)$ (in a_0^{-1})	$S_2'(R_B)$ (in a_0^{-1})	$S_4'(R_B)$ (in a_0^{-1})	$S_2'(R_C)$ (in a_0^{-1})	$S_4'(R_C)$ (in a_0^{-1})
-0.0275	-0.0138	-0.0233	-0.0127	-0.0350	-0.0180
B_2^0, cm^{-1}		B_4^0, cm^{-1}		B_4^4, cm^{-1}	
$40374 + 3426G$		$6444 + 9818G$		$4307G$	

*) a_0 is the Bohr radius

Numerical values of the overlap integrals $S_l(R_C), S_l(R_B), S_l(R_C)$ (Table 2) were computed with the aid of the radial 3d wave functions of Mn^{III} and $2s, 2p$ functions of oxygen and nitrogen given in [32]. The parameters B_2^0, B_4^0, and B_4^4 as functions of the parameter *G* were estimated with the aid of formulae (6), (8) and the overlap integrals, they are also listed in Table 2. In fact, this representation allows determining the partial contributions that come to the parameters B_l^m from the exchange and point charges of the crystal field. Further on the value of the parameter G will be obtained from the optimal coincidence between the calculated and observed temperature dependence of the magnetic susceptibility and effective magnetic moment.

Finally, let us focus on the problem of the basis set. The crystal field of C_{2v} symmetry (Eq.(7)) acting on the manganese ions may produce significant splitting of the cubic terms of the Mn^{III} ions thus changing the mutual arrangement of levels. In this field, the $hs{-}^5E(t_2^3e)$ term splits into two nondegenerate states which are not mixed with any other state by Coulomb

interaction since the configuration d^4 gives only one cubic *E*-level with the spin *S*=2. On the other hand, the configurations $t_2^4, t_2^3e, t_2^2e^2, t_2e^3$ give rise to seven $^3T_1$ levels [33]. To properly reproduce the energies of the low-lying Stark levels arising from the splitting of the $ls-^3T_1(t_2^4)$ term, we include the following states in the basis set:

$$^3T_1(t_2^4), ^3T_1(t_2^3(^2T_2)e), ^3T_1\ (t_2^3(^2T_1)e), ^3T_1\ (t_2^2(^3T_1)e^2(^1A_1)), ^3T_1(t_2^2(^3T_1)e^2(^1E)), ^3T_1(t_2^2(^3T_1)e^2(^3A_2)), \quad ^3T_1\ (t_2e^3) \tag{9}$$

and take into account the interaction of these states with the crystal field (7) as well as their Coulomb mixing [33].The wavefunctions of states (9) are quoted in the Appendix. Since the Racah parameters in a crystal are reduced as compared to those for free ions due to the covalency of the bonds manganese(III)-ligand (the so-called nephelauxetic effect, see for instance, [34]) in calculations we take values which make up 80% of the free ion values for the parameters B and C.

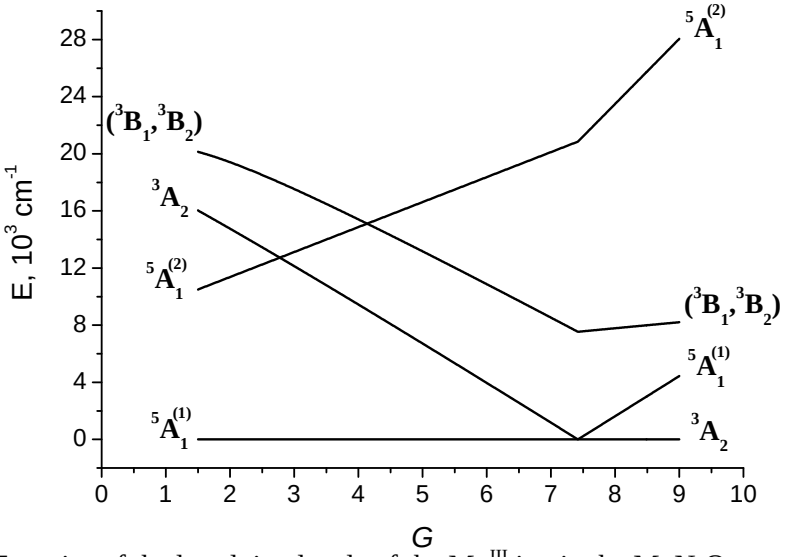

Fig. 2. Energies of the low-lying levels of the Mn^{III} ion in the MnN_4O_2 complex as functions of the exchange charge model parameter *G*.

The calculations apparently show that, in a wide range of parameter *G* values, the effect of mixing of the $^3T_1(t_2^4)$ state with the other six $^3T_1$ states (9) is comparatively small for the Mn^{III} ion in the mixed ligand surrounding, and the low-lying energy spectrum of this ion consists of four levels predominantly arising from the splitting of the $^3T_1(t_2^4)$ and $^5E(t_2^3e)$ states by the crystal field (Fig. 2). These levels transform according to the irreducible representations $A_2, (B_1, B_2)$, $A_1^{(1)}, A_1^{(2)}$ of the C_{2v} point group (Fig. 2), the energies of the states $^3B_1$ and $^3B_2$ coincide. It is seen from Fig. 2 that, for parameter G values less than 2.78, the ground is the $^5A_1^{(1)}$ level while the first excited is the $^5A_1^{(2)}$ level. With increase of G, the energy of the state $^3A_2$ becomes lower than that of the $^5A_1^{(2)}$ state, but the ground state remains the same. At the point $G = 7.42$, a change in the ground state takes place. In the range of parameters $G > 7.42$, the ground $^3A_2$ and the excited $^5A_1^{(1)}$ states belong to spin values S=1 and S=2, respectively. The range of parameters $G > 7.42$ is favorable for spin-crossover in the $[MnL2]NO_3$ compound. It should be also noted that, in the

range of parameters G wherein spin crossover may take place (Fig. 2), the energy gaps between the excited $({}^3B_1, {}^3B_2)$, ${}^5A_1^{(2)}$ and the low-lying ${}^3A_2$ and ${}^5A_1^{(1)}$ levels significantly exceed kT. Thus, the low-lying spectrum consists of two levels *ls*-${}^3A_2$ and *hs*-${}^5A_1^{(1)}$ well separated from other excited levels arising from the splitting of the cubic ${}^3T_1$ and ${}^5E$ terms.

2.2.Electron-deformational interaction

Taking into account that the spin transformation in the compound under examination does not cause a change in crystal symmetry, the spontaneous strain accompanying the spin conversion is assumed to be full symmetric and to appear as a consequence of the occupation of the antibonding e - orbital in the Mn^{III} ion. Since the medium between the molecules in spin-crossover compounds is more easily affected by deformation than that inside the molecule, a difference is made between the intramolecular and intermolecular space in the subsequent examination. As in [35, 36], we introduce the internal molecular $\varepsilon_1 = (\varepsilon_{xx}^1 + \varepsilon_{yy}^1 + \varepsilon_{zz}^1)/\sqrt{3}$ and external (intermolecular volume) $\varepsilon_2 = (\varepsilon_{xx}^2 + \varepsilon_{yy}^2 + \varepsilon_{zz}^2)/\sqrt{3}$ strains and bulk moduli c_1 and c_2 corresponding to these full symmetric strains. In each molecule, we consider the interaction of the Mn^{III} –ion with the arising ε_1 strain. In accordance with the Kanamori's approach [37], the contribution of uniform strains ε_1 and ε_2 in the crystal Hamiltonian can be set by the operator

$$H_{st} = \frac{Nc_1\Omega_0\varepsilon_1^2}{2} + \frac{Nc_2(\Omega - \Omega_0)\varepsilon_2^2}{2} + \nu_1\varepsilon_1\sum_n \tau_n + \nu_2\varepsilon_1 N\,, \tag{10}$$

where Ω_0 and Ω are the molecular and unit cell volumes, respectively, N is the number of unit cells in the crystal, $\nu_1 = (\nu_{hs} - \nu_{ls})/2, \nu_2 = (\nu_{hs} + \nu_{ls})/2$, ν_{hs} and ν_{ls} are the constants of interaction of the Mn^{III} ion with the full symmetric strain ε_1 in the $hs - {}^5A_1^{(1)}$ and $ls - {}^3A_2$ states, respectively. In Eq.(10) the first two terms describe the elastic energy of the deformed crystal, the third and the fourth terms correspond to the coupling of the d electrons of the Mn^{III} ion with the uniform deformation ε_1. In the basis of the *hs* and *ls* states, the matrix τ_n is of the dimension 8x8 and has the following form:

$$\tau_n = \begin{pmatrix} 1 & 0 & 0 & 0 & 0 & 0 & 0 & 0 \\ 0 & 1 & 0 & 0 & 0 & 0 & 0 & 0 \\ 0 & 0 & 1 & 0 & 0 & 0 & 0 & 0 \\ 0 & 0 & 0 & 1 & 0 & 0 & 0 & 0 \\ 0 & 0 & 0 & 0 & 1 & 0 & 0 & 0 \\ 0 & 0 & 0 & 0 & 0 & -1 & 0 & 0 \\ 0 & 0 & 0 & 0 & 0 & 0 & -1 & 0 \\ 0 & 0 & 0 & 0 & 0 & 0 & 0 & -1 \end{pmatrix} \tag{11}$$

The diagonal matrix elements of τ_n equal to 1 and –1 correspond to the *hs* and *ls* states, respectively. For a uniform crystal compression (or extension), the relation of ε_2 to ε_1 is roughly

supposed to be

$$\varepsilon_2 \approx \varepsilon_1 \frac{c_1}{c_2}. \tag{12}$$

If we replace the intramolecular and intermolecular volumes by coupled parallel springs, the same relation will hold. With account of Eq.(12) after minimizing Eq.(10) over the strain ε_1 we find

$$H_{st} = -b\sum_n \tau_n - \frac{J}{2N}\sum_{n,m}\tau_n\tau_m, \tag{13}$$

where $b = Av_1v_2$, $J = Av_1^2$, $A = \dfrac{c_2}{c_1[c_2\Omega_0 + c_1(\Omega - \Omega_0)]}$. Thus, the coupling to the strain gives rise to an infinite-range interaction between all manganese ions of the crystal. It should be mentioned that the model of the elastic continuum, above introduced, satisfactorily describes only the long-wave acoustic vibrations of the lattice. Therefore, the obtained intermolecular interaction in fact corresponds to the exchange via the field of long-wave acoustic phonons. The first term in Eq.(13) also arises from the interaction with the deformation and acts as an additional field applied to each spin-crossover molecule.

2.3. Mean field approximation

For a system of interacting spin-crossover manganese ions the solution of the problem can be obtained in the framework of the mean field approximation. Within the framework of this approximation we reduce the problem of interacting spin-crossover molecules to the one-center problem substituting $\tau_n\tau_m$ in the interaction Hamiltonian (13) with

$$\tau_n\tau_m = \bar{\tau}\tau_m + \tau_n\bar{\tau} - \langle\tau\rangle^2, \tag{14}$$

where $\bar{\tau} = \langle\tau\rangle = Tr(\rho\tau_n)$ and $\rho = Exp(-H/kT)/Tr(Exp(-H/kT))$ is the density operator for the spin-crossover system, H is the total Hamiltonian of the crystal. The Hamiltonian H_{st} decomposes into the sum of single-ion Hamiltonians

$$\tilde{H}_{st} = \sum_n H_{st}^n,\ H_{st}^n = -(B + J\bar{\tau})\sum_n \tau_n\ . \tag{15}$$

Then, taking into account Eq.(15), we obtain the total Hamiltonian for a single Mn^{III} -ion

$$H_n = H_{st}^n + \frac{\Delta}{2}\tau_n\ , \tag{16}$$

where Δ is the crystal field gap between the *hs*-$^5A_1^{(1)}$ and *ls*-$^3A_2$ states (Fig. 2) The eigenvalues of the Hamiltonian H_n are $\varepsilon_{hs} = \dfrac{\Delta}{2} - B - J\bar{\tau}$, $\varepsilon_{ls} = -\dfrac{\Delta}{2} + B + J\bar{\tau}$. Using the eigenvalues of the Hamiltonian H_n as a basis set, we obtain the following expression for the free energy of a single manganese ion in the molecular field:

$$F(T) = -kT\ln\left[(gExp(-(\Delta_{hs} - J(2n_{hs} - 1))/kT) + Exp(-J(2n_{hs} - 1)/kT)\right] - \frac{\Delta_{hs}}{2}$$
$$- kT\ln g_{ls} + J(2n_{hs} - 1)^2/2 \tag{17}$$

where n_{hs} is the $hs-$fraction or the total population of the $hs-$state connected with the mean value of the order parameter by the relation $2n_{hs}-1=\bar{\tau}$, and $\Delta_{hs} = \Delta - 2b$ is the effective gap between the hs and ls states in the presence of cooperative interaction. It is seen that the parameter $-2b$ only redefines the crystal field gap Δ. Finally, $g = g_{hs}/g_{ls}$, g_{hs} and g_{ls} are the degeneracies of the hs and ls states, respectively. The two states have different degeneracies because of the different spin multiplicities and the different density of vibrational states associated with them [38, 39]. The entropy change ΔS is connected with the ratio g_{hs}/g_{ls} by the relation $\Delta S = R\ln g_{hs}/g_{ls}$ [40]. This change upon conversion is noticeable and contains vibrational contributions [41, 42].

Minimizing the free energy $F(T)$ per one crossover manganese ion over n_{hs}, we obtain a self-consistent equation for the hs -fraction:

$$\frac{gExp(-(\Delta_{hs} - J(2n_{hs} - 1))/kT) - Exp(-J(2n_{hs} - 1)/kT)}{gExp(-(\Delta_{hs} - J(2n_{hs} - 1))/kT) + Exp(-J(2n_{hs} - 1)/kT)} = 2n_{hs} - 1. \tag{18}$$

The obtained equation for the hs -fraction has a set of non-trivial solutions determined by different relations between the characteristic internal parameters of the system.

3. Magnetic properties

The energy levels in the mean field approximation and the temperature dependence of the *hs*-fraction are used for calculation of the magnetic moment of the manganese complex with the aid of the Van Vleck formula

$$\mu^2 = g_S^2\mu_B^2 \frac{6gExp(-\varepsilon_{hs}/kT) + 2Exp(-\varepsilon_{ls}/kT)}{gExp(-\varepsilon_{hs}/kT) + Exp(-\varepsilon_{ls}/kT)}. \tag{19}$$

The temperature dependence of the magnetic susceptibility can be easily obtained from the relation

$$\mu = \sqrt{8\chi T}\ . \tag{20}$$

In the calculation of the magnetic susceptibility, the parameter of the electron deformational interaction *J* was estimated by the method suggested in [43]. This estimation gave the value $J = 95\,cm^{-1}$. At the same time, the effective gap Δ_{hs} and the ratio $g = g_{hs}/g_{ls}$ were considered as fitting parameters.

Figure 3 displays the observed temperature dependence of the magnetic susceptibility over the temperature range of 50-300 K. The experimental room temperature value of χ is $8.22\cdot10^{-3}$ cm^3mol^{-1} [21] and decreases to $6.92\cdot10^{-3}$ cm^3mol^{-1} as the temperature is lowered to 175 K, after which temperature χ monotonically increases. A fairly good agreement between the observed and calculated curves of the magnetic susceptibility is obtained. The best fit is achieved for the parameter values $\Delta_{hs} = 395\,cm^{-1}$ and $g = 10$. With the same set of parameters Δ_{hs} and g ,

the variation of the effective magnetic moment as a function of temperature was calculated (Fig. 4). It is seen that the model under examination also reproduces the observed magnetic moment curve. The low temperature value of the magnetic moment corresponds to the spin $S=1$. However, the observed magnetic moment value 4.36 μ_B at 293 K is lower than 4.9 μ_B thus testifying that the spin conversion in the compound under examination is not complete.

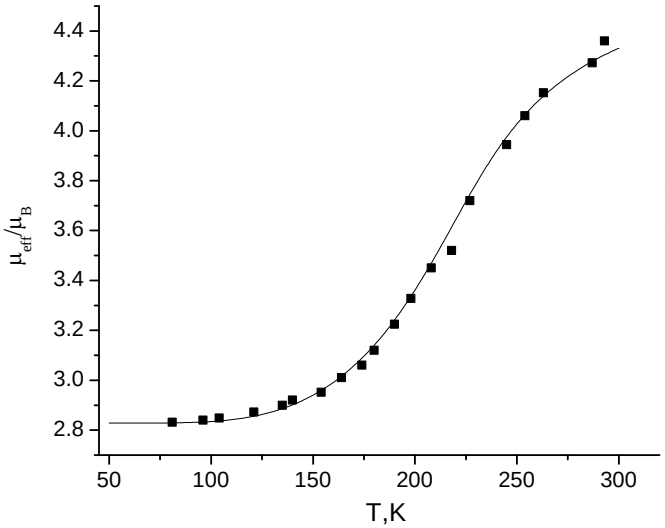

Fig. 3. Variation of the effective magnetic moment of the [MnL2]NO_3 compound as a function of temperature. Squares are experimental data [15]; solid lineis theoretical fit with $g=10$, $\Delta_{hs}=395cm^{-1}$, $J=95cm^{-1}$.

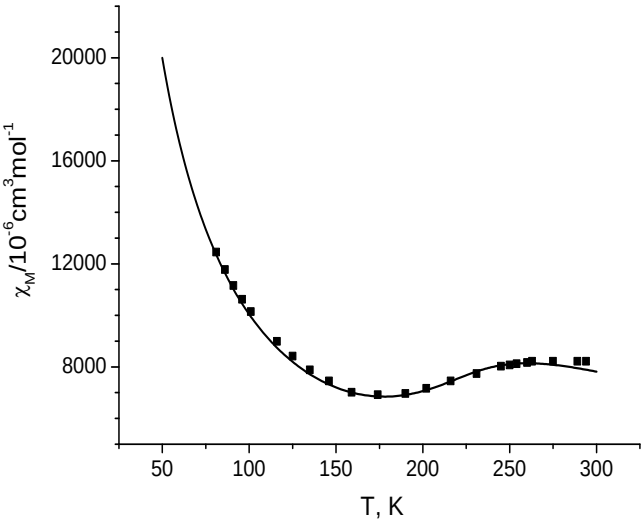

Fig. 4. Temperature dependence of the magnetic susceptibility for the [MnL2]NO_3 compound. Squares are experimental data [15]; solid line is theoretical fit with $g=10$, $\Delta_{hs}=395cm^{-1}$, $J=95cm^{-1}$.

Since experimental data on the entropy change ΔS accompanying the spin transition in the [MnL2]NO_3 compound are not available, we estimated the ratio $g=g_{hs}/g_{ls}$ from the observed value $\Delta S=13.8JK^{-1}mol^{-1}$ for manganese(III) spin crossover compounds, such as [Mn(taa)] (H3taa = tris(1-(2-azolyl)-2-azabuten-4-yl)amine) and [Mn^{III}(pyrol)$_3$tren] [18, 23]. The value $g=5.3$ calculated from ΔS [23] is approximately 1.9 times lower than that obtained from the fitting procedure for [MnL2]NO_3. Meanwhile, the parameter g is an intrinsic characteristic of the compound and even depends on the concentration of the spin crossover ions [44]. This allows assuming that the best fit value $g=10$ is reasonable. The obtained g value is much lower than those for Fe^{II} spin crossover compounds [44] and shows that, for the Mn^{III} systems, not all metal-ligand stretching vibrations contribute to ΔS. This result is in accordance with the estimate of the vibrational contribution to the entropy change associated with the spin transition in d^4 systems performed in [23].

4. Concluding remarks

To explain the phenomenon of spin transition in the $[MnL2]NO_3$ compound, we report a theoretical model. The model takes into account the low symmetry crystal field acting on the manganese ion and the cooperative long-range electron-deformational interaction facilitating the spin transition. The inputs for the task are: the structure of the complex formed by the manganese ion and its nearest surrounding, the crystal structure and experimental data concerning the magnetic properties. The main results of the consideration can be summed up in the following way. An energy level diagram is constructed for a single Mn^{III} ion in the mixed ligand surrounding of C_{2v} symmetry. The energies of the levels are calculated in the exchange–charge model of the crystal field accounting for covalence effects. The range of the crystal field parameters for which the low-lying part of the energy spectrum of the Mn^{III} ion consists of two non-degenerate levels arising from the states $^3T_1$ and ^5E with the spin S=1 state being the ground one is determined. It is shown that, in this case, the ground level mainly originates from the $^3T_1$ (t_2^4) term; that is, the situation facilitating the spin crossover takes place. Cooperative long-range interactions are shown to arise from the coupling of the electronic states of the Mn^{III} ion to the full symmetric strain. In this case, the molecular field theory has proved particularly successful. Fairly good agreement is obtained between the calculated and experimental values of the magnetic susceptibility and effective magnetic moment. It should be underlined that the model developed is also applicable for consideration of other manganese complexes that exhibit spin crossover.

Acknowledgments

I would like to earnestly thank my scientific advisor Sophia Klokishner for her support and willingness to discuss all my questions and all my problems. Also, I thank Dr. Oleg Reu for his most helpful suggestions in programming.

References

[1] O. Kahn, J. Kröber, and C. Jay, Adv. Mater., 4, 718, (1992).
[2] M. Nakano, G. Matsubayashi, and T. Matsuo, Advances in Quantum Chemistry, 44, 617, (2003).
[3] Y. Garcia, V. Ksenofontov, and P. Gütlich, Hyperfine Interactions, 139/140, 545, (2002).
[4] L. Cambi, L. Szego, and A. Cagnasso, Atti accad Lincei, 13, 168, (1931).
[5] L. Cambi and L. Szego, Atti accad Lincei, 15, 329, (1931**).**
[6] L. Cambi and L. Szego, Atti accad Lincei, 15, 599. (1932).
[7] P. Gütlich, A.Hauser, and H. Spiering, Angew. Chem., Int. Ed. Engl, 33, 20, (1994).
[8] P. Gütlich, Y. Garcia, and H. A. Goodwin, Chem. Soc. Rev, *29*, 419, (2000).
[9] A. Hauser, Coord. Chem. Rev., 111, 275, (1991).
[10] P. Gütlich and H. A. Goodwin, Spin Crossover in Transition Metal Compounds, Springer-Verlag, (2004).
[11] A.Hauser, Light-Induced Spin Crossover and the High-Spin → Low-Spin Relaxation; Springer-Verlag, (2004).
[12] P. Gütlich,; V. Ksenofontov, and A.B. Gaspar, Coord. Chem. Rev.**,** 249, 1811, (2005).

[13] P.G. Sim and J. Sinn, J. Am. Chem. Soc., 103, 241, (1981).
[14] D.M. Halepoto, D.G.L.Holt, L.F.Larkworthy, G.L.Leigh, D.C.Povey, and G.W.Smith, J.Chem.Soc.Chem.Commun.**,**1322, (1989).
[15] K.S.Murray, Eur.J.Inorg.Chem.**,** 3101, (2008).
[16] Y.Garcia and P.Gütlich, Topics in Current Chemistry**,** 234, 786, (2004).
[17] P.Greig Sim and E. Sinn, J. Am. Chem. Sos., 103 (1), 241-243, (1981).
[18] Y. Garsia, O. Kahn, J-P. Ader, A. Buzdin, Y. Meurdesoif, and M. Guillot, Phys. Lett. A, 271, 145, (2000).
[19] M. Nakano, G. Matsubayshi, and T. Matsuo, Phys. Rev. B, 66, 212412, (2002).
[20] S. Kimura, Y.Narumi, D.Kindo, M. Nakano, and G.Matsubayshi, Phys. Rev. B**,** 72, 064448, (2005).
[21] G.G. Morgan, K.D. Murnaghan, H. Müller-Bunz, V. McKee, and C.J. Harding, Angew. Chem. Int. Ed., 45,7192, (2006).
[20] S. Wang, M. Ferbinteanu, C. Marinescu, A. Dobrinescu, Q.-D. Ling, and W. Huang, Inorg. Chem., 49, 9839, (2010).
[23] Y.Garsia, H. Paulsen, V. Schünemann, A.X.Trautwein, and J. A. Wolny, Phys. Chem. Chem. Phys., 9,1194, (2007).
[24] I. B. Bersuker, The Jahn-Teller Effect and Vibronic Interactions in Modern Chemistry, Plenum: New York-London,(1984).
[25] M.N. Popova, E.P. Chukalina, B.Z. Malkin, and S.K. Saikin, Phys. Rev. B. 61, 7421, (2000).
[26] S. Klokishner, J. Melsheimer, F.C. Jentoft, and R. Schlögl, Phys. Chem. Chem. Phys., 6, 2066, (2004).
[27] S.I. Klokishner, B.S. Tsukerblat, O.S. Reu, A.V. Palii, and S.M. Ostrovsky, Chem. Phys., 316, 83, (2005).
[28] S.I. Klokishner, B.S.Tsukerblat, O.S. Reu, A.V. Palii, and S.M. Ostrovsky, Optical Materials, 27,1445, (2005).
[29] S.I.Klokishner, O.S. Reu, S.M. Ostrovsky, A.V. Palii, L.L. Kulyuk, B.S. Tsukerblat, and E. Towe, J. Mol. Str., 838, 133. (2007).
[30] S. Klokishner, O. Reu, S. Ostrovsky, A. Palii, and E.Towe, J. Phys.: Condens. Matter, 19, 486213, (2007).
[31] A. Abragam and B. Bleaney, Electron paramagnetic resonance of transition ions; Clarendon Press: Oxford, (1970**)**.
[32] E. Clementi and C. Roetti, At.Data Nucl.Data Tables, 14.177, (1974).
[33] S. Sugano, Y. Tanabe, and H. Kamimura, Multiplets of transition metal Ions in crystals, Academic, Press: New York and London, (1970).
[34] S.W. Biernach, A. Kaminska, A. Suchocki, and L. Arizmendi, Applied Phys. Letters, 81, 442, (2002).
[35] S.I. Klokishner, F. Varret, and J. Linares, Chem. Phys., 255, 317, (2000).
[36] S.I. Klokishner and J. Linares, Phys. Chem. C., 111, 10644, (2007).
[37] J. Kanamori, J. Appl. Phys., 31, 145, (1960).
[38] A. Bousseksou, F. Varret, and J. Nasser, J. Physique, 3**,** 1463, (1993).
[39] A. Bousseksou, H.Constant-Machado, and F. Varret, J. Physique I, 5 747, (1995).
[40] C. P. Slichter and H. G. Drickamer J. Chem. Phys.**,** 56, 2142, (1972).
[41] M.Sorai and S. Seki, J. Phys. Chem. Solids, 35**,** 5550, (1974).
[42] A.Bousseksou, J. McGarvey, F. Varret, J. A. Real, J. P. Tuchagues, A .C. Dennis, and M. L. Boillot, Chem. Phys. Lett, 318**,** 409, (2000).

[43] S. Klokishner, Chem. Phys., 269, 411, (2001).
[44] C. Enachescu, J. Linares, and F. Varret, J. Phys.: Condens. Matter, 13 , 2481, (2001).

Appendix

Wavefunctions of the ${}^3T_1(t_2^n e^m)$ $(n+m=4)$ terms

${}^3T_1\ (t_2^4)$

$$\left|{}^3T_{1\alpha}\right\rangle = -\left|\zeta\xi\bar{\xi}\eta\right|,\ \left|{}^3T_{1\beta}\right\rangle = \left|\xi\eta\bar{\eta}\zeta\right|,\left|{}^3T_{1\gamma}\right\rangle = \left|\eta\zeta\bar{\zeta}\xi\right|$$

${}^3T_1\ (t_2^3({}^2T_2)e)$

$$\left|{}^3T_{1\alpha}\right\rangle = -\frac{\sqrt{3}}{2\sqrt{2}}\left|\xi\eta\bar{\eta}u\right| - \frac{\sqrt{3}}{2\sqrt{2}}\left|\xi\zeta\bar{\zeta}u\right| - \frac{1}{2\sqrt{2}}\left|\xi\eta\bar{\eta}v\right| - \frac{1}{2\sqrt{2}}\left|\xi\zeta\bar{\zeta}v\right|,$$

$$\left|{}^3T_{1\beta}\right\rangle = \frac{\sqrt{3}}{2\sqrt{2}}\left|\eta\xi\bar{\xi}u\right| + \frac{\sqrt{3}}{2\sqrt{2}}\left|\eta\zeta\bar{\zeta}u\right| - \frac{1}{2\sqrt{2}}\left|\eta\xi\bar{\xi}v\right| - \frac{1}{2\sqrt{2}}\left|\eta\zeta\bar{\zeta}v\right|,$$

$$\left|{}^3T_{1\gamma}\right\rangle = \frac{1}{\sqrt{2}}\left|\zeta\xi\bar{\xi}v\right| + \frac{1}{\sqrt{2}}\left|\zeta\eta\bar{\eta}v\right|$$

${}^3T_1\ (t_2^3({}^2T_1)e)$

$$\left|{}^3T_{1\alpha}\right\rangle = -\frac{1}{2\sqrt{2}}\left|\xi\eta\bar{\eta}u\right| + \frac{1}{2\sqrt{2}}\left|\xi\zeta\bar{\zeta}u\right| + \frac{\sqrt{3}}{2\sqrt{2}}\left|\xi\eta\bar{\eta}v\right| - \frac{\sqrt{3}}{2\sqrt{2}}\left|\xi\zeta\bar{\zeta}v\right|$$

$$\left|{}^3T_{1\beta}\right\rangle = \frac{1}{2\sqrt{2}}\left|\eta\xi\bar{\xi}u\right| - \frac{1}{2\sqrt{2}}\left|\eta\zeta\bar{\zeta}u\right| + \frac{\sqrt{3}}{2\sqrt{2}}\left|\eta\xi\bar{\xi}v\right| - \frac{\sqrt{3}}{2\sqrt{2}}\left|\eta\zeta\bar{\zeta}v\right|$$

$$\left|{}^3T_{1\gamma}\right\rangle = \frac{1}{2\sqrt{2}}\left|\zeta\xi\bar{\xi}u\right| - \frac{1}{2\sqrt{2}}\left|\zeta\eta\bar{\eta}u\right|$$

${}^3T_1\ (t_2^2({}^3T_1)e^2({}^1A_1))$

$$\left|{}^3T_{1\alpha}\right\rangle = \frac{1}{\sqrt{2}}\left|\bar{\eta}\bar{\zeta}u\bar{u}\right| + \frac{1}{\sqrt{2}}\left|\bar{\eta}\bar{\zeta}v\bar{v}\right|,\left|{}^3T_{1\beta}\right\rangle = \frac{1}{\sqrt{2}}\left|\bar{\zeta}\ \bar{\xi}u\bar{u}\right| + \frac{1}{\sqrt{2}}\left|\bar{\zeta}\ \bar{\xi}v\bar{v}\right|,\left|{}^3T_{1\gamma}\right\rangle = \frac{1}{\sqrt{2}}\left|\bar{\xi}\bar{\eta}u\bar{u}\right| + \frac{1}{\sqrt{2}}\left|\bar{\xi}\bar{\eta}v\bar{v}\right|.$$

${}^3T_1\ (t_2^2({}^3T_1)e^2({}^1E))$

$$\left|{}^3T_{1\alpha}\right\rangle = -\frac{1}{2\sqrt{2}}\left|\eta\zeta u\bar{u}\right| + \frac{1}{2\sqrt{2}}\left|\eta\zeta v\bar{v}\right| + \frac{\sqrt{3}}{2\sqrt{2}}\left|\eta\zeta u\bar{v}\right| + \frac{\sqrt{3}}{2\sqrt{2}}\left|\eta\zeta v\bar{u}\right|,$$

$$\left|{}^3T_{1\beta}\right\rangle = \frac{1}{2\sqrt{2}}\left|\zeta\xi u\bar{u}\right| - \frac{1}{2\sqrt{2}}\left|\zeta\xi v\bar{v}\right| - \frac{\sqrt{3}}{2\sqrt{2}}\left|\zeta\xi u\bar{v}\right| + \frac{\sqrt{3}}{2\sqrt{2}}\left|\zeta\xi v\bar{u}\right|,$$

$$\left|{}^3T_{1\gamma}\right\rangle = -\frac{1}{\sqrt{2}}\left|\xi\eta u\bar{u}\right| + \frac{1}{\sqrt{2}}\left|\xi\eta v\bar{v}\right|.$$

$^3T_1\ (t_2^2(^3T_1)e^2(^3A_2))$

$$\left|{}^3T_{1\alpha}\right\rangle=\frac{1}{\sqrt{2}}\left|\eta\bar{\zeta}uv\right|+\frac{1}{\sqrt{2}}\left|\zeta\bar{\eta}uv\right|,\left|{}^3T_{1\beta}\right\rangle=\frac{1}{\sqrt{2}}\left|\zeta\,\bar{\xi}uv\right|+\frac{1}{\sqrt{2}}\left|\xi\bar{\zeta}uv\right|,\left|{}^3T_{1\gamma}\right\rangle=\frac{1}{\sqrt{2}}\left|\xi\bar{\eta}uv\right|+\frac{1}{\sqrt{2}}\left|\eta\bar{\xi}uv\right|$$

$^3T_1\ (t_2e^3)$

$$\left|{}^3T_{1\alpha}^{(7)}\right\rangle=-\frac{\sqrt{3}}{2}\left|u\bar{v}v\xi\right|-\frac{1}{2}\left|v\bar{u}u\xi\right|,\quad\left|{}^3T_{1\beta}^{(7)}\right\rangle=\frac{\sqrt{3}}{2}\left|u\bar{v}v\eta\right|-\frac{1}{2}\left|v\bar{u}u\eta\right|,\ \left|{}^3T_{1\gamma}^{(7)}\right\rangle=\left|v\bar{u}u\zeta\right|$$

$^5E(t_2^3e)$

$$\left|{}^5E_u\right\rangle=-\left|\xi\eta\zeta v\right|,\ \left|{}^5E_v\right\rangle=\left|\xi\eta\zeta u\right|$$

Matrix elements of the crystal field operator in the basis of the $^3T_1$ states

$^3T_1\ (t_2^4)$

$$\left\langle{}^3T_{1\alpha}\left|V_{cr}\right|{}^3T_{1\alpha}\right\rangle=388-5458\cdot G,\left\langle{}^3T_{1\beta}\left|V_{cr}\right|{}^3T_{1\beta}\right\rangle=388-5458\cdot G,\left\langle{}^3T_{1\gamma}\left|V_{cr}\right|{}^3T_{1\gamma}\right\rangle=-4387-5856\cdot G.$$

$^3T_1\ (t_2^3(^2T_1)e)$

$$\left\langle{}^3T_{1\alpha}\left|V_{cr}\right|{}^3T_{1\alpha}\right\rangle=-2419-2534\cdot G,\left\langle{}^3T_{1\beta}\left|V_{cr}\right|{}^3T_{1\beta}\right\rangle=-2419-2534\cdot G,\left\langle{}^3T_{1\gamma}\left|V_{cr}\right|{}^3T_{1\gamma}\right\rangle=3485-1222\cdot G.$$

$^3T_1\ (t_2^3(^2T_2)e)$

$$\left\langle{}^3T_{1\alpha}\left|V_{cr}\right|{}^3T_{1\alpha}\right\rangle=1517-1659\cdot G,\left\langle{}^3T_{1\beta}\left|V_{cr}\right|{}^3T_{1\beta}\right\rangle=1517-1659\cdot G,\left\langle{}^3T_{1\gamma}\left|V_{cr}\right|{}^3T_{1\gamma}\right\rangle=-4387-2971\cdot G.$$

$^3T_1\ (t_2^2(^3T_1)e^2(^1A_1))$

$$\left\langle{}^3T_{1\alpha}\left|V_{cr}\right|{}^3T_{1\alpha}\right\rangle=-1291+1265\cdot G,\left\langle{}^3T_{1\beta}\left|V_{cr}\right|{}^3T_{1\beta}\right\rangle=-1291+1265\cdot G,\left\langle{}^3T_{1\gamma}\left|V_{cr}\right|{}^3T_{1\gamma}\right\rangle=3485+1663\cdot G.$$

$^3T_1\ (t_2^2(^3T_1)e^2(^1E))$

$$\left\langle{}^3T_{1\alpha}\left|V_{cr}\right|{}^3T_{1\alpha}\right\rangle=-1291+1265\cdot G,\left\langle{}^3T_{1\beta}\left|V_{cr}\right|{}^3T_{1\beta}\right\rangle=-1291+1265\cdot G,\left\langle{}^3T_{1\gamma}\left|V_{cr}\right|{}^3T_{1\gamma}\right\rangle=3485+1663\cdot G.$$

$^3T_1\ (t_2^2(^3T_1)e^2(^3A_2))$

$$\left\langle{}^3T_{1\alpha}\left|V_{cr}\right|{}^3T_{1\alpha}\right\rangle=-1291+1265\cdot G,\left\langle{}^3T_{1\beta}\left|V_{cr}\right|{}^3T_{1\beta}\right\rangle=-1291+1265\cdot G,\left\langle{}^3T_{1\gamma}\left|V_{cr}\right|{}^3T_{1\gamma}\right\rangle=3485+1663\cdot G.$$

$^3T_1\ (t_2e^3)$

$$\left\langle{}^3T_{1\alpha}\left|V_{cr}\right|{}^3T_{1\alpha}\right\rangle=677+4587\cdot G,\left\langle{}^3T_{1\beta}\left|V_{cr}\right|{}^3T_{1\beta}\right\rangle=677+4587\cdot G,\left\langle{}^3T_{1\gamma}\left|V_{cr}\right|{}^3T_{1\gamma}\right\rangle=1805+5502\cdot G.$$

$^5E(t_2^3\ e)$

$$\left\langle{}^5E_u\left|V_{cr}\right|{}^5E_u\right\rangle=-4387-2971\cdot G,\left\langle{}^5E_v\left|V_{cr}\right|{}^5E_v\right\rangle=3485-1222\cdot G.$$